Proceedings of LPM2010 - the 11th International Symposium on Laser Precision Microfabrication,
7-11 June 2010, Stuttgart, Germany

Laser processing for advanced solar cells

Jochen Löffler, Laurie Wipliez, Wim Soppe, Martijn de Keijzer, Johan Bosman,
Machteld Lamers, Agnes Mewe, Arthur Weeber, Ian Bennett, Paul de Jong

Energy Research Centre of The Netherlands, P.O. Box 1, 1755 ZG Petten, The Netherlands
E-mail: loffler@ecn.nl

Laser processing is becoming an increasingly important production tool in the manufacturing of photovoltaic (PV) solar cells and modules, with huge potential to enable new technology generations in the near future. In this contribution, examples of next generation crystalline silicon and thin-film PV devices that are developed by ECN will be presented. These incorporate laser processes, ranging from a highly thermal process like laser soldering, via drilling of holes into silicon up to precise micrometer scale selective ablation of nanometer thin films. The presented next generation PV solutions enabled by laser processing are characterized by an overall advantage in device performance and/or substantial decrease in manufacturing cost through overall optimization of the complete concept and its production scheme. Depth–selective laser ablation is an enabler for ECN's high-efficiency thin-film silicon PV approach which has the potential to allow a significant decrease in production cost through roll-to-roll manufacturing based on steel foil as substrate. In case of crystalline silicon, the combination of laser drilled metallisation wrap-through solar cells with an innovative module technology for such back-contacted solar cells enabled a 17% module efficiency with multicrystalline silicon solar cells, which is listed in the table of PV world record efficiencies [1].

Keywords: Solar cell, LASER, drilling, thin film ablation, soldering, crystalline silicon, thin film silicon

1. Introduction

Recent energy supply and market studies [2,3,4] agree on the tremendous growth scenarios for photovoltaics (PV), predicting a fast increase of the share of this technology in an overall increasing energy supply. This will lead to a continued double-digit growth of installed PV capacity per year worldwide, which can only be achieved with an increasing production capacity that will grow towards capacities of 50 - 160 GW_p/year over the coming decade, equivalent to an area in the order of 100000 square kilometers of produced PV panels per year.

The demand for lasers and laser systems by the PV industry will increase at a probably even higher rate, as the assumed cost decrease for photovoltaic electricity is based on the expected development of high-efficiency solar cells and modules with low material consumption. This can be achieved by advanced device concepts based on crystalline silicon, which often involve innovative laser processes, and by a further development of thin-film PV concepts, that rely on laser technology for monolithic series connection and edge deletion. In addition to this, the fast development in the field of laser technology may lead to another significant market for retrofitting or upgrading existing PV production lines.

We present here a general overview of the laser processing needs for the next generations of crystalline silicon wafer based solar cells and modules, and focus on two technologies developed at ECN: metallization wrap-through solar cells with laser drilled vias, and the accompanying back contact module technology including in-laminate soldering.

For the area of thin-film PV, we present the concept and latest results of depth selective laser scribing for monolithic series interconnection enabling low-cost high-efficiency thin-film silicon solar cells for roll-to-roll production on steel foil. This concept can be extended to any thin-film technology manufactured in this way.

2. Crystalline silicon PV

A conventional 'first generation' crystalline Silicon solar cell is sketched in Figure 1. It is basically a planar diode consisting of a p–doped silicon wafer with a negatively doped area at the top from where the sunlight enters, and a positively doped area at the rear. To collect the current from the front surface, a metal grid with distance between the fingers of a few mm is applied. Two or three wider metal lines (busbars) are applied orthogonally to the grid lines in order to extract the current with low electrical losses. A typical size of such a solar cell wafer is 156x156 mm^2. In order to fabricate a PV panel of 1-2 m^2 from such solar cells, they have to be connected in series. This can be done by soldering so-called tabs between the cells, connecting the front contact (busbars) of one cell to the rear of the next cell, thus forming a 'string'. These strings are further connected in series or in parallel, and then the whole assembly is encapsulated by lamination between glass and a back sheet foil, with EVA as encapsulant.

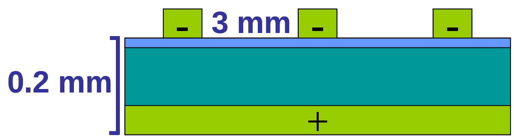

Figure 1. Standard 'H-pattern' solar cell.

This type of solar cells and modules is the current workhorse of PV industry, but can in principle be improved on the following points:
- Reduced shading losses from metallization and tabs at the front surface
- Thinner wafers to reduce material cost, requiring a low-stress interconnection between cells
- Reduced resistance losses due to tabs
- Easier manufacturing of modules

2.1 Laser processing for next generations of crystalline silicon PV

It is foreseen that the above mentioned points for improvement will be introduced in an evolutionary way, passing through the technology generations sketched in Figure 2.

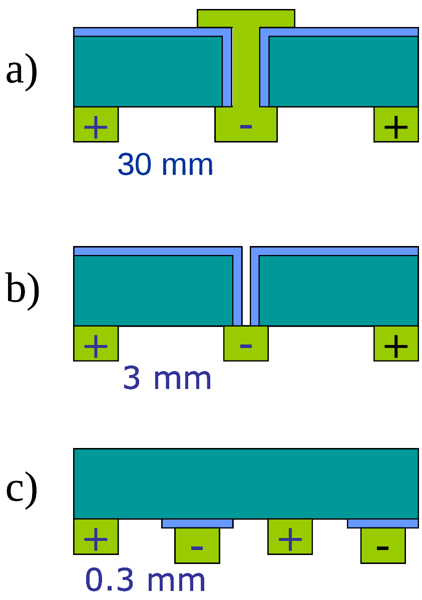

Figure 2. Next generations of crystalline silicon solar cells: a) metallization wrap-through (MWT), b) emitter wrap-through (EWT) and c) interdigitated back contacted cells (IBC). The typical dimensions of a ‘unit cell’, i.e. distance between positive and negative electrodes, is indicated.

Common to all these concepts is that both electrodes are placed at the rear, allowing advanced interconnection schemes as presented below, which combine the reduction of resistance losses, mechanical stresses and also the inactive area between the individual cells in a module, while at the same time enabling easier, thus more cost-effective manufacturing.

The metallization wrap-through cell is a first step in reducing shading losses, by omitting the busbars of the standard cells, and instead leading all the generated current through thin gridlines towards laser drilled vias. These vias are also filled with metal, thus leading the front electrode to contact points at the rear. A typical pattern of this metallization with 16 vias (optimized at ECN) is shown in Figure 3.

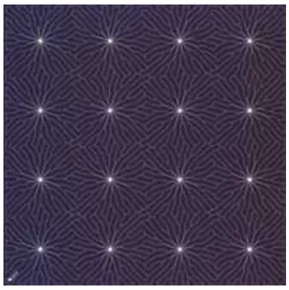

Figure 3. Typical metallization wrap-through solar cell with 16 vias and grid pattern optimized by ECN*.

For MWT, depending on the size of the solar cell and the exact layout of the contact pattern, 16 to 100s of vias have to be laser drilled with a typical throughput of 1 wafer per second.

An even more advanced concept is EWT (emitter-wrap-through) that fully eliminates all metal from the front surface of the solar cell. In the EWT solar cells, the current is guided by the negatively doped area (emitter) at the front surface towards and through vias to contact points at the rear. The disctance between the vias has to be reduced to a few mm due to the lower conductivity of the emitter. Therefore, 10000s of holes have to be drilled into the wafer with a throughput of 1 wafer per second. This still presents a challenge for current laser systems

An even higher efficiency potential has the interdigitated-back contact cell (IBC), which has no vias. All positively and negatively doped areas are placed at the rear of the solar cell. Traditionally, this type of cell has to rely on costly lithography techniques in order to generate the sub-mm patterns for the two different types of doped areas. Laser processes could be applied to realize such cells in a more economic way [5] e.g. by local opening of diffusion masks or by local laser doping. These processes require far less pulse energy than drilling of holes into silicon wafers, but large part of the wafers (up to 50% or more) have to be scanned with sub-mm resolution, again at a throughput in the order of 1 cell per second. Another important challenge here is to minimize laser induced damage in the silicon material.

2.2 Laser processing for metallization wrap-through solar cells and modules

The required vias for MWT solar cells have a diameter of 50-500 µm and are generally produced by trepanning. Different drilling processes have been developed ranging from nanosecond ablation till melt ejection processes, up to ≤ ms pulse length. The ablation dominated process leads to vias with slight rim formation on the side where the laser hits the wafer due to recast and melt displacement, and very smooth edges at the bottom of the via. For the discussed melt ejection process the molten material is actually expelled at the bottom of the via, leaving the edge at the top of the wafer smooth, with a clear rim at the bottom.

The process of choice for the overall concept has to be tailored to the full device and module processing scheme, taking into account the compatibility with processing steps

* Solland Solar Energy Holding BV is the owner of the registered industrial designs Sunweb®

before and after the laser step. Finally, optimization of the overall process has to lead to maximum performance and yield in terms of mechanical stability as well as efficiency.

The main advantages of MWT cells and module include reduced shadowing at the front of the cell due to the lack of front contacts and tabs. Additionally the cells can be placed closer together in the module as no tabs need to pass between the front and rear of the cell. The conductive components of the module can be wider than conventional tabbing material because they are not limited in width as there are no shadowing losses. There is also no need for bussing at the top and bottom of the module so increasing the effective area. The cell design and module layout can be integrated and optimised simultaneously with respect to module output and total costs. For example, the number of contacts between the rear of the cell and the conductive components of the module can be optimised for both cell and module efficiency.

To fully benefit from the advantages of MWT cells, an alternative module manufacturing technology can be employed. At ECN, a method using a patterned conductive foil as the module substrate was developed [6], see Figure 4. The foil is similar to a standard TPT back-sheet foil with an additional inner layer consisting of a conductive sheet. The conductive sheet is patterned to match the contact points on the rear of the back-contact cell. This results in a series interconnection of the cells on the foil. The cells are placed on the foil using a method analogous with pick-and-place technology used for SMD in the electronics industry. This reduces cell handling to just one gentle pick-and-place step so limiting potential damage to the cells.

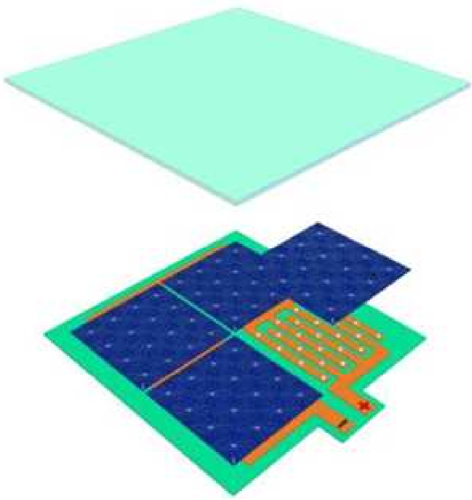

Figure 4. Module concept for back-contacted solar cells with low-resisitive pattern in backsheet foil, and compatibility with pick-and place technology for cell alignment.*

The actual connection between the contact points of the cell and the conductive pattern of the backsheet foil can be realized by in-laminate laser soldering (ILS) [7]. The process sequence is depicted in Figure 5, and consists of the application of solder material and placing of the solar cells followed by the encapsulation with a cover glass connected to the cells and the backsheet foil by EVA under heat and pressure in a vacuum laminator. The actual electrical connection is made by soldering *after* the fabrication of the laminate. This is realized by local heating of the solder points by a laser, thus forming a robust metallic joint between solar cell and conductive track in the back sheet foil.

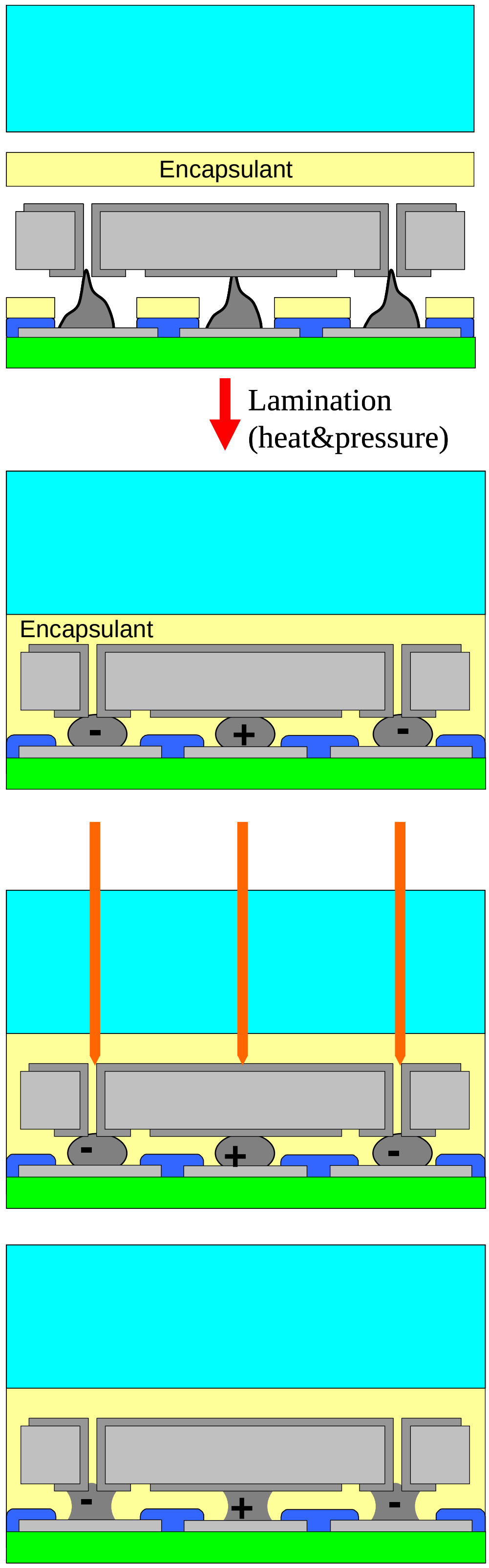

Figure 5. Process sequence for in-laminate laser soldering.

* Solland Solar Energy Holding BV is the owner of the registered industrial designs Sunweb®

As reported recently [8], by optimization of the solar cells, the module layout, and the overall layouts and processes, ECN has obtained an efficiency of 17% [9] for a full-size module with MWT solar cells based on multicrystalline silicon wafers and the advanced back contact module technology. This result is listed in the table of PV world record efficiencies [1] and has been obtained with interconnections by conductive adhesives, but the comparable electrical quality of solder joints obtained by ILS suggests the possibility to obtain similar results also with ILS.

3. Thin-film silicon PV

Thin film amorphous/microcrystalline silicon tandem solar cells (so-called 'micromorph cells') are an emerging PV technology as a cheap alternative to the more traditional wafer-based crystalline silicon solar cells since they can be produced using low-cost manufacturing methods. An inherent advantage of thin-film PV technology is the ability to directly produce series interconnected modules on the substrate by laser structuring the PV active layers into stripes (leaving the substrate as carrier intact) which are monolithically series interconnected during the further device processing. Recently, many production lines for thin-film silicon PV modules based on glass substrates have become operational. Production capacity is expanded worldwide as turn-key fabrication equipment for this technology is available on the market, including the laser scribing tools and processes. However, the applied interconnection processes require three separate deposition steps (for TCO, silicon layers, and rear contact, respectively), each of which is followed by a laser scribing step in atmosphere [10]. This implies several handling steps of the glass substrates, and pump-down cycles for the vacuum deposition equipment both adding considerably to the manufacturing cost.

Therefore, an important further decrease in production cost is expected when moving to high-throughput roll-to-roll (R2R) production, where handling is limited to coils carrying kilometers of substrate foil which is further processed to PV laminates in more compact production tools requiring less floor space. Besides, roll-to-roll production of thin film Si solar cells has several further advantages over batch-type reactor systems, for instance the opportunity to make lightweight and flexible products. Flexible and lightweight PV modules gear up to building integrated PV: the most important market for PV in densely populated, developed countries [11, 12].

However, in contrast to production lines based on glass substrates, no standard equipment is currently available for R2R production of thin-film silicon solar cells and modules. For the series interconnection, no standard concept has emerged yet, although some manufacturers are working on proprietary solutions.

To overcome these limitations, ECN is currently developing the technology and setting up a pilot line for the production of low-cost and high-efficiency tandem solar cells based on microcrystalline and amorphous silicon on steel foil substrates [13]. To allow monolithic series interconnection on these electrically conducting substrates, an insulating barrier layer is required. On top of this barrier layer, a sputtered back contact is applied, followed by PECVD of the silicon layers and the front TCO sputtering. In order to further reduce the substrate handling during the manufacturing, in the ECN concept first all solar cell layers are deposited, and then the monolithic series interconnection is realized in one single process step by three depth selective laser scribes (P1, P2, and P3) which are subsequently filled by insulating and electrically conductive inks, see Figure 6.

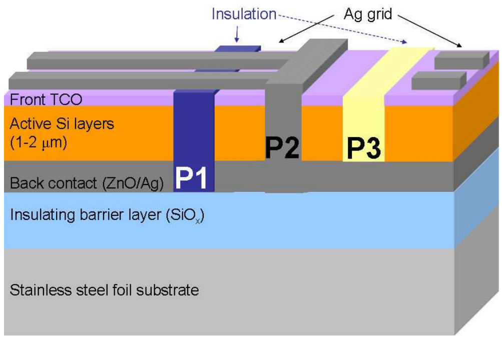

Figure 6. Thin-film silicon PV Module concept on electrically insulated steel foil substrate.

P1 has the function to separate the cells from each other electrically. Thus, all the layers of the full cell have to be ablated here, including the back contact. The main challenge is to have no remaining bridges of the back contact between two adjacent cells in the scribe, while the insulating layer should be unaffected. The laser scribe P2 is necessary for the actual connection of the front contact of one cell to the back contact of the adjacent cell. This scribe should remove all silicon layers, but leave the ZnO/Ag back contact unaffected. The insulating scribe P3 can in principle be obtained with the same process as P2. We describe below the current status of process development for depth selective laser scribing towards fully integrated monolithic modules.

3.1 Depth-selective laser ablation for high-efficiency thin-film silicon PV modules on flexible substrates

Laser scribing experiments have been performed with nanosecond pulsed diode pumped solid- state YAG lasers mainly at 355 nm and 1064 nm, equipped with galvo-head scanners to guide the laser over the substrates resulting in locally isolated spots, or, when overlapping subsequent spots, in continuous lines. Besides the direct parameters scanner speed, laser frequency and the pump diode current, the output power could also be directly controlled by an external attenuator.

To gain more insight into the selectivity of the ablation process, the ablation thresholds of the different layers involved have been determined. Then, the laser parameters have been systematically varied, yielding a pulse energy / spot overlap matrix. Also multi-pass scribing, (2 or more scribing lines on top of each other) has been investigated.

The resulting laser spots and scribes have been analysed by optical microscopy, confocal microscopy, SEM and EDX. The samples for laser processing consisted of the layer stack (or part of the stack) as shown in Figure 6 and were fabricated by spray-coating of a thermally curing SiO_x based sol-gel lacquer on stainless steel foil substrates, followed by magnetron sputtering of Ag and ZnO:Al layers. Then, amorphous and microcrystalline Si layers were deposited by PECVD. As front TCO, 80 nm of ITO have been applied by RF magnetron sputtering.

From conceptual considerations, an ideal depth-selective ablation process would be ‘self-regulating’ in depth, e.g. because of differences in absorption and/or thermo-mechanical properties of the involved layers. A good example for such a ‘self-regulating’ process is the removal of a silicon layer from a TCO/glass substrate [10] with a green laser, which is practically not absorbed by the TCO, so that a clean removal of the Si from the TCO can be obtained.

For the P1 scribe of the interconnection concept presented here, one has to take into account that the investigated laser wavelengths are absorbed very effectively in the steel substrate. Potential damage or even ablation of the substrate surface is critical as it may induce damage to the insulating barrier layer. Thus, despite the high transparency of the barrier layer itself, the P1 scribing process cannot be self-regulating and has to be optimized to just ablate the back contact, with minimal exposure of the barrier layer and back contact to the laser radiation.

For the P2/P3 scribes, when neglecting the absorption in the TCO layers, the most critical selectivity is expected between the silicon layers and the Ag layer in the back contact. In first instance, the 355 nm wavelength appeared most interesting for these scribes, as the silicon layers show very high absorption even exceeding the values for the Ag layer. The small optical penetration depth in silicon at this wavelength allows for careful control of the ablated material volume per laser pulse by tuning the pulse energy. For the analysis and understanding of the ablation process the Gaussian intensity profile is used as an important property of the laser pulses. Assuming a certain ablation threshold H_s (in J/cm^2) and a diameter of the Gaussian beam in focus d_f, the resulting ablation spot will have a diameter d_{abl} which increases with increasing laser fluence H following equation (1).

$$d_{abl} = d_f \sqrt{\frac{1}{2} \ln \frac{H}{H_S}} \qquad (1)$$

Solving this equation for the ablation threshold H_s allows the determination of this specific parameter by varying the pulse energy of the laser and measuring the corresponding ablation diameters d_f:

$$H_S = H \exp\left(-2 \left(\frac{d_{abl}}{d_f} \right)^2 \right) \qquad (2)$$

Figure 7 shows the dependence of the ablation diameter on the pulse energy for the back contact and the silicon layers. For the same optical configuration, we found that the ablation threshold for the back contact without silicon layer on top is with a value of 0.125 J/cm^2 only ¼ of the threshold for the ablation of the Si layer which amounts to approximately 0.5 J/cm^2.

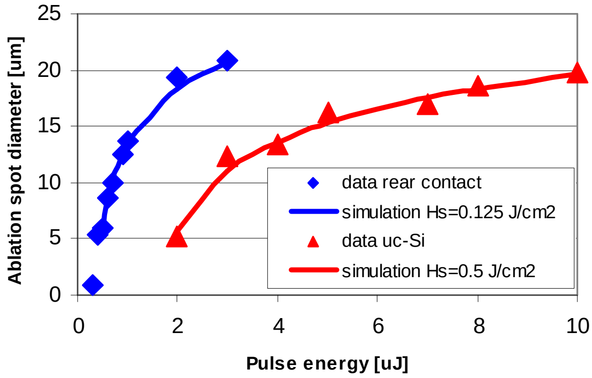

Figure 7. Ablation diameter versus pulse energy for the back contact and the µc-Si layer. Fitting of these curves yields the ablation thresholds of the corresponding layers for the 355 nm laser.

Thus, the removal of the silicon layers from the back contact at a laser wavelength of 355 nm is not a self-regulating process. Only slightly too high pulse energy will lead to a removal of the back contact together with the silicon layers. Consequently, the scribing depth has to be controlled by the laser process itself (i.e. pulse energy, spot overlap, etc). The process window for a clean removal of only the silicon from the back contact is rather narrow, see Figure **8**. At only slightly too large or too little pulse energy or spot overlap, locally either the back contact is removed, or Si remains that bridges the scribe. Scribing in multiple passes did not improve the quality of the scribes, nor could we increase the process window.

	2 µJ	4 µJ
Too shallow	 Pulse overlap 74 %	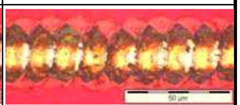 Pulse overlap 62 %
Optimum	 Pulse overlap 76 %	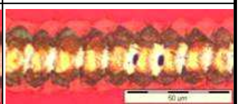 Pulse overlap 64 %
Too deep	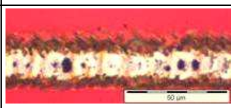 Pulse overlap 78 %	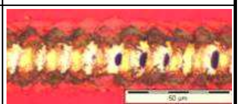 Pulse overlap 66 %

Figure 8. Pulse energy / pulse overlap combinations to achieve P2 scribes with the UV ns laser.

With the same 355 nm laser, a robust P1 scribe can be accomplished straightforwardly, for example in single or double pass mode, as shown in Figure 9.

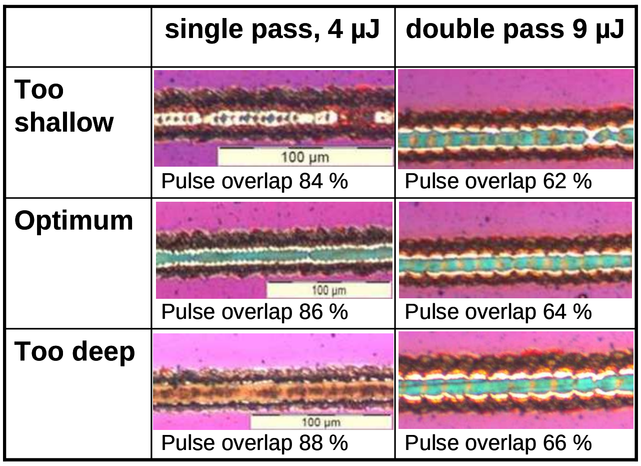

Figure 9. Pulse energy / pulse overlap combinations to achieve P1 scribes with the UV ns laser in single and double pass

In search of a larger process window especially for the P2 scribe, also 532 nm and 1064 nm lasers have been applied and actually all scribes (P1, P2, P3) have been realized on stacks including either amorphous or microcrystalline silicon on top of the steel / barrier / back contact samples [14]. In the following, we focus on the results obtained with the 1064 nm laser. Excellent P1 and P2 scribes of the complete stack, including ITO deposited on the (amorphous) silicon, were obtained as shown in Figure 10 and Figure 11, respectively. In both pictures, the optimum scribes can be found in the center.

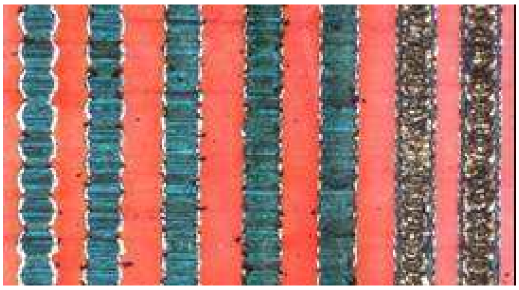

Figure 10. P1 scribes obtained with a 1064 nm ns pulsed laser. From left to right the spot overlap was increased

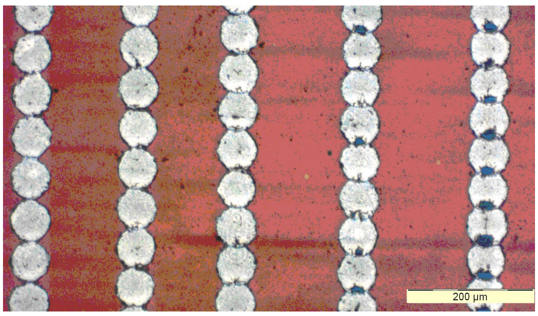

Figure 11. P2 scribes obtained with a 1064 nm ns pulsed laser. From left to right the spot overlap was increased.

It has to be mentioned that also with this laser, the process window especially for the P2 scribe is quite narrow, as can be deduced from ablation threshold experiments similar to those presented for the 355 nm laser above. Figure 12 shows the ablation diameters of only the back contact as function of the pulse energy, together with the diameters obtained on the 'full stack' samples for the two different ablation depths representing the P1 and P2 scribes. Also here, the risk of damaging the back contact during P2 scribing cannot be eliminated.

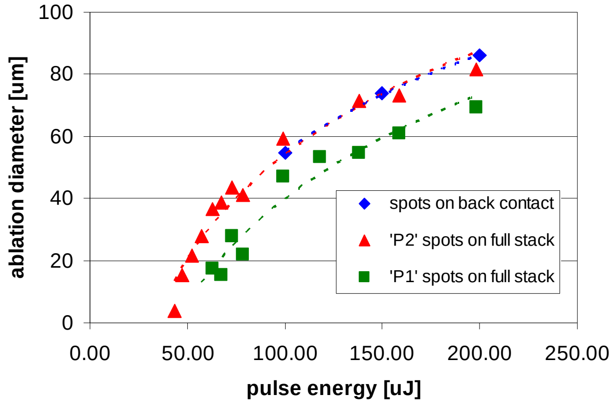

Figure 12. Diameter of ablation versus pulse energy with 1064 nm laser.

When judging the quality of the obtained scribe lines presented in Figure 10 and Figure 11, an important observation is that the SiO_x layer still has a very flat surface after laser scribing of P1, indicating that there is no significant damage to this layer. This is confirmed by a closer analysis of the confocal microscopy results presented in Figure 13.

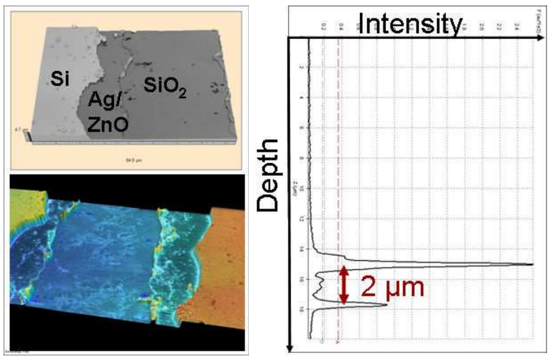

Figure 13. Confocal microscopy analysis of the P1 laser scribe.

The confocal microscope actually finds a strong signal for all reflecting interfaces that are present in the stack during the measurement. As the SiO_x layer is transparent, the surface of the steel substrate and the surface of the insulating layer are visible in the P1 scribe. The appearance of these two peaks confirms the complete removal of the non-transparent back contact, and the distance of 2 µm between the peaks indicates the unchanged thickness of the insulating layer.

An important observation for the P2 scribe is that obviously the back contact remains fully unaffected at places where the silicon and ITO are removed. In EDX analysis, we found Zn in the P2 scribes, and a Zn/Ag ratio comparable to the value outside the scribe. This indicates that the ZnO is still present on top of the easily visible Ag layer.

A possible explanation for the initially unexpected selective ablation obtained at 1064 nm is an ablation mechanism governed by pressure induced ejection, where the pressure may be built up by the silicon layer itself, e.g. due to the formation of hydrogen gas as a result of heating [15], or by the expansion of the rear contact.

The best laser scribing parameters have also been tested in functional solar cells. For these experiments, a similar approach as presented in [10] has been chosen, scribing only part of a small test solar cell, and evaluating the device performance before and after the laser steps.

In first instance issues with short-circuiting of the solar cells have been observed, which could be explained by recast and displaced back contact material connecting the front ITO and rear metal contact of the solar cell. In the meantime, a more detailed study involving also other lasers in a broader wavelength, pulse length, and beam shape matrix has been performed, and this shunting issue could be minimized. Details will be published elsewhere [16].

4. Conclusions and outlook

Laser processing can play a crucial role in enabling the commercial production of future generations of crystalline silicon wafer based as well as thin-film PV technology. For both technology families, the overall device and manufacturing concept has to be optimized with respect to performance and cost, rather than focusing on and evaluating only one individual (e.g. laser) processing step.

An example of such concepts for next generation crystalline silicon wafer based technology are metallization wrap-through solar cells with laser drilled vias and the accompanying back contact module technology which can be realized by laser soldering. A module efficiency of 17%, listed in the table of world records, has been obtained recently with a back-contact module employing MWT cells at ECN. This concept is currently transferred to industrial mass production; laser processes for again new technology generations are under investigation.

For the development of thin-film silicon modules on steel foil, depth selective laser scribing has been demonstrated as one of the key enablers for this low-cost high-efficiency approach. Initial issues with shunting from recast of the rear contact have been minimized and first solar cell results with virtually no losses in electrical performance due to the laser process have been achieved. In a next step, the device concept including full monolithic series interconnection by laser scribing and subsequent printing of insulating and conductive inks will be demonstrated.

Acknowledgments

Part of this work was funded by the European Commission under contract nrs. SES6-CT-2003-502583 (Integrated Project Crystal Clear) and EU FP-6 Energy 2004 – 019948 (FLEXCELLENCE), and by the Dutch Ministry of Economic Affairs (contract TSIN3043).

We would like to thank Matthias Fahland (Fraunhofer Institute FEP Dresden, Germany) for supplying the sputtered Ag / ZnO:Al layers, and Claudia Finck and Michael Wutz (Rofin) for the fruitful cooperation on part of the presented laser process development.

The companies Solland Solar, REC and Q-Cells are acknowledged for their contributions.

References

[1] M.A. Green, K. Emery, Y. Hishikawa and W Warta, Prog. Photovolt: Res. Appl., 18, (2010) 144–150.

[2] EU Strategic Energy Technology (SET) Plan: *SET for 2020 – Solar Photovoltaic Electricity: A mainstream power source in Europe by 2020*, www.setfor2020.eu (2009).

[3] International Energy Agency, *Technology Roadmap Photovoltic Solar Energy*, http://www.iea.org (2010).

[4] European Photovoltaic Industry Association (EPIA), *Global market outlook for photovoltaics until 2014, May 2010 update*, http://www.epia.org (2010).

[5] D. M. Huljić et al., Proc. 21st EU PVSEC, Dresden, Germany (2006).

[6] P. C. de Jong, D. W. K. Eikelboom, R. Kinderman, A. C. Tip, J. H. Bultman, M. H. H. Meuwissen, M. A. C. J. van den Nieuwenhof, Proc. 19th EU PVSEC, Paris, France, (2004).

[7] Patent WO2009NL50534.

[8] I.J. Bennett, C. Tjengdrawira, A.A. Mewe, M.W.P.E. Lamers, P.C. de Jong and A.W. Weeber, Proc. 24th EU PVSEC, Hamburg, Germany (2009).

[9] M.W.P.E. Lamers et al., to be published.

[10] S. Haas, A. Gordijn, H. Stiebig, Prog. Photovolt: Res. Appl. 16, (2008) 195.

[11] M. Izu, and T. Ellison, Sol. En. Mat. Sol. Cells 78, (2003) 613.

[12] A. Takano, and T. Kamoshita, Jap. J. Appl. Phys. 43, (2004) 7976.

[13] B.B. van Aken, M. Dörenkämper, C. Devilee, M.C.R. Heijna, J. Löffler, and W.J. Soppe, Proc. IEEE PVSC Philadelphia (2009).

[14] J. Löffler, L.A. Wipliez, M.A. de Keijzer, J. Bosman, W.J. Soppe, Proc. IEEE PVSC Philadelphia (2009).

[15] W. Shinohara, M. Shima, S. Taira, K. Uchihashi, A. Terakawa, in Proceedings of SPIE Vol. 6107, 61070J (2006) 1-18.

[16] J. Löffler, L.A. Wipliez, M.A. de Keijzer, A. Schoonderbeek, O. Haupt, R. Kling, J. Bosman, and W.J. Soppe, to be presented at 28th ICALEO, Anaheim, CA, USA (2010).